

Site-disorder driven superconductor-insulator transition: A dynamical mean field study

Naushad Ahmad Kamar and N. S. Vidhyadhiraja

Theoretical Sciences Unit

Jawaharlal Nehru Centre for Advanced Scientific Research,

Jakkur, Bangalore 560 064, India.

Abstract

We investigate the effect of site-disorder on the superconducting (SC) state in the attractive Hubbard model within the framework of dynamical mean field theory. For a fixed interaction strength (U), the SC order parameter (OP) decreases monotonically with increasing disorder (x), while the single-particle spectral gap (SG) decreases for small x , reaches a minimum and keeps increasing for larger x . Thus, the system remains gapped beyond the destruction of the superconducting state, indicating a disorder-driven superconductor-insulator transition. We investigate this transition in depth considering the effects of weak and strong disorder for a range of interaction strengths. In the clean case, the order-parameter is known to increase monotonically with increasing interaction, saturating at a finite value asymptotically for $U \rightarrow \infty$. The presence of disorder results in destruction of superconductivity at large U , thus drastically modifying the clean case behaviour. A physical understanding of our findings is obtained by invoking particle-hole asymmetry and the probability distributions of the order parameter and spectral gap.

PACS numbers: 74.62.Dh, 74.20.Pq, 74.81.-g

I. INTRODUCTION

The combined effect of disorder and correlations on the superconducting state has been extensively studied since many decades but a complete picture has not emerged yet [1, 2]. Many recent experimental studies of disordered superconducting thin films have investigated the superconductor-insulator transition (SIT) [3–5]. In disordered NbN s-wave superconductors [3, 4], an SIT was observed through scanning tunneling spectroscopy and penetration depth measurements. The effective disorder in NbN, given by the product of Fermi wave vector (k_F) and electronic mean free path (l), is introduced by controlling the vacancy of Nb atoms. The insulating state at large disorder has been a subject of debate. Finite frequency measurements of superfluid stiffness [5] have indicated the existence of a Bose insulator state with localized Cooper pairs. However, a better understanding of the SIT and the associated insulating state in the large disorder limit requires more theoretical scrutiny.

Localized Cooper pairs indicate a system with local attractive interactions, which are most appropriately represented by the attractive Hubbard model (AHM). The study of dirty superconductors can thus be naturally carried out by investigating the effect of disorder in the attractive Hubbard model. The clean limit of the AHM has been extensively studied using Bogoliubov-de Gennes type mean field (BdGMF) theories and more recently using iterated perturbation theory with superconducting bath (IPTSC) [6], numerical renormalization group (NRG) [7] and continuous time quantum Monte Carlo (CTQMC) [8] within dynamical mean field theory (DMFT) [9–11]. The main issue that has been focused on is the BCS-BEC crossover for different fillings and interaction strengths. Very recently, a statistical-DMFT study of the Bethe lattice disordered AHM has been carried out [12].

The systems investigated experimentally, such as NbN_x [3, 4] and InO_x [5] are in the strong disorder limit, wherein the early theories of dirty superconductors, e.g by Anderson [13] and by Abrikosov and Gorkov [14] are not really applicable. Hence a proper theoretical approach is needed which treats the effects of strong attractive interactions and disorder on an equal footing. One such method, namely the BdGMF has been employed to investigate the AHM with site[15] as well as bond disorder [16]. However, the method, being based on a mean field approximation, albeit inhomogeneous, has limitations in terms of not incorporating quantum fluctuations. Recent NRG [7] calculations of the clean AHM also point out several deficiencies of the BdGMF method. Beyond mean field, QMC [17] studies of finite size

lattices have validated the decrease of superconducting order parameter (Φ) with increasing disorder, but due to finite size effects, a complete destruction of Φ at large disorder could not be seen. However, with increasing temperature, a superconductor-insulator transition was observed in the dc conductivity calculations.

In this work, we carry out a detailed study of the disordered AHM by combining coherent potential approximation (CPA) [18, 19], with DMFT and iterated perturbation theory for superconductivity (IPTSC). The IPTSC solver has the advantage over methods such as QMC of obtaining real frequency spectra at zero temperature and in the thermodynamic limit, while being computationally inexpensive. The reliability of our approach is enhanced by the fact that the IPTSC is known to benchmark well with NRG results for the clean AHM. To distinguish between dynamical and static effects, we have also carried out BdGMF studies within CPA+DMFT. As anticipated by the previous inhomogeneous mean field and QMC calculations, we find a SIT with increasing disorder. We map out the detailed behaviour of the SIT in the disorder-interaction plane. We also investigate the distribution of the local order parameter, and point out that some of the subtle aspects of the experimentally observed SIT require an extension of single-site DMFT through e.g the statistical DMFT or cluster extensions such as the dynamical cluster approximation. The paper is structured as follows: In the following section, we outline the model and the formalism used. Next, we present our results for the local order parameter, the spectra, the distribution of the order parameter and the phase diagram. We conclude in the final section.

II. MODEL AND FORMALISM

The attractive Hubbard model (AHM) is expressed, in standard second quantized notation by the following Hamiltonian:

$$\mathcal{H} = \sum_{i\sigma} \epsilon_i c_{i\sigma}^\dagger c_{i\sigma} - t \sum_{\langle ij\sigma \rangle} \left(c_{i\sigma}^\dagger c_{j\sigma} + h.c \right) - |U| \sum_i n_{i\uparrow} n_{i\downarrow} - \mu \sum_{i\sigma} c_{i\sigma}^\dagger c_{i\sigma} \quad (1)$$

where $c_{i\sigma}$ annihilates an electron on i^{th} lattice site with spin σ , and $n_{i\sigma} = c_{i\sigma}^\dagger c_{i\sigma}$; t is nearest-neighbour hopping amplitude, ϵ_i is site-energy, and μ is chemical potential. The disorder is represented by randomness in site energies, which we choose to be distributed according to

a uniform probability distribution function $P_\epsilon(\epsilon_i)$,

$$P_\epsilon(\epsilon_i) = \frac{\Theta(\frac{x}{2} - |\epsilon_i|)}{x} \quad (2)$$

where x is disorder strength in unit of t ($= 1.0$).

The CPA in conjunction with DMFT is the best single-site approach to study the interplay of disorder with interactions in strongly correlated systems [20]. To investigate the effects of disorder on the superconducting state, we employ the best single-site quantum approaches, namely DMFT in conjunction with CPA. Within DMFT, the lattice model is mapped onto a single-impurity model embedded in a self-consistently determined bath. For the present problem, the effective medium is in a superconducting state, hence the Nambu formalism must be used. The impurity Green's function in Nambu formalism is given as

$$\hat{G}^i{}^{-1}(\omega^+) = \begin{pmatrix} \omega^+ + \mu - \epsilon_i - \Delta_{11}(\omega^+) - \Sigma_i(\omega^+) & -\Delta_{12}(\omega^+) - S_i(\omega^+) \\ -\Delta_{21}(\omega^+) - S_i(\omega^+) & \omega^+ - \mu + \epsilon_i - \Delta_{22}(\omega^+) + \Sigma_i^*(-\omega^+) \end{pmatrix} \quad (3)$$

where $\Delta_{\alpha\beta}$, $\alpha, \beta = 1, 2$ are components of the disorder-averaged hybridisation function matrix $\hat{\Delta}$, Σ_i and S_i are normal and anomalous self-energies of the i^{th} site respectively.

To calculate the local self-energies, $\Sigma_i(\omega^+)$ and $S_i(\omega^+)$ for the i^{th} site, we use iterated perturbation theory for superconductivity (IPTSC)[6] as the impurity solver. In the IPTSC method, based on second order perturbation theory, the self-energies are given by the following ansatz:

$$\Sigma_i(\omega^+) = -U \frac{n_i}{2} + A_i \Sigma_i^{(2)}(\omega^+) \quad (4)$$

$$S_i(\omega^+) = -U \Phi_i + A_i S_i^{(2)}(\omega^+) \quad (5)$$

where the local filling n_i and order parameter Φ_i are given by

$$n_i = -\frac{2}{\pi} \text{Im} \int_{-\infty}^{\infty} d\omega G_{11}^i(\omega^+) f(\omega) \quad (6)$$

$$\Phi_i = \int_{-\infty}^{\infty} d\omega \frac{-\text{Im} G_{12}^i(\omega^+)}{\pi} f(\omega) \quad (7)$$

and $f(\omega) = \theta(-\omega)$ is the Fermi-Dirac distribution function at zero temperature. In the

ansatz above (equations (4,5)), the second order self-energies are given by

$$\begin{aligned}\Sigma_i^{(2)}(\omega^+) &= U^2 \int_{-\infty}^{\infty} \prod_{j=1}^3 d\omega_j \frac{g_{1i}(\omega_1, \omega_2, \omega_3) N(\omega_1, \omega_2, \omega_3)}{\omega^+ - \omega_1 + \omega_2 - \omega_3} \\ &\text{and} \\ S_i^{(2)}(\omega^+) &= U^2 \int_{-\infty}^{\infty} \prod_{j=1}^3 d\omega_j \frac{g_{2i}(\omega_1, \omega_2, \omega_3) N(\omega_1, \omega_2, \omega_3)}{\omega^+ - \omega_1 + \omega_2 - \omega_3},\end{aligned}\quad (8)$$

where

$$\begin{aligned}N(\omega_1, \omega_2, \omega_3) &= f(\omega_1)f(-\omega_2)f(\omega_3) + f(-\omega_1)f(\omega_2)f(-\omega_3) \\ g_{1i}(\omega_1, \omega_2, \omega_3) &= \tilde{\rho}_{11}^i(\omega_1)\tilde{\rho}_{22}^i(\omega_2)\tilde{\rho}_{22}^i(\omega_3) - \tilde{\rho}_{12}^i(\omega_1)\tilde{\rho}_{22}^i(\omega_2)\tilde{\rho}_{12}^i(\omega_3) \\ g_{2i}(\omega_1, \omega_2, \omega_3) &= \tilde{\rho}_{12}^i(\omega_1)\tilde{\rho}_{12}^i(\omega_2)\tilde{\rho}_{12}^i(\omega_3) - \tilde{\rho}_{11}^i(\omega_1)\tilde{\rho}_{12}^i(\omega_2)\tilde{\rho}_{22}^i(\omega_3)\end{aligned}\quad (9)$$

and the spectral functions $\tilde{\rho}_{\alpha\beta}^i$, $\alpha, \beta = 1, 2$ are given by the imaginary part of the ‘Hartree-corrected’ host Green’s function, namely $\hat{\rho}_i = -\text{Im}\hat{\mathcal{G}}^i/\pi$. The latter is given by

$$\hat{\mathcal{G}}^i(\omega^+)^{-1} = \begin{pmatrix} \omega^+ + \mu - \epsilon_i - \Delta_{11}(\omega^+) + U\frac{n_i}{2} & -\Delta_{12}(\omega^+) + U\Phi_i \\ -\Delta_{21}(\omega^+) + U\Phi_i & \omega^+ - \mu + \epsilon_i - \Delta_{22}(\omega^+) - U\frac{n_i}{2} \end{pmatrix}. \quad (10)$$

Finally the coefficient A_i in the IPTSC ansatz (equation (4,5), which is determined by the high frequency limit is given by

$$A_i = \frac{\frac{n_i}{2}(1 - \frac{n_i}{2}) - \Phi_i^2}{\frac{n_{0i}}{2}(1 - \frac{n_{0i}}{2}) - \Phi_{0i}^2}, \quad (11)$$

where the pseudo order-parameter Φ_{0i} and the pseudo occupancy n_{0i} are given by

$$\begin{aligned}n_{0i} &= 2 \int_{-\infty}^{\infty} d\omega \tilde{\rho}_{11}^i(\omega) f(\omega) \\ \text{and } \Phi_{0i} &= \int_{-\infty}^{\infty} d\omega \tilde{\rho}_{12}^i(\omega) f(\omega)\end{aligned}\quad (12)$$

Using the coherent potential approximation (CPA) for incorporating disorder, the CPA Green’s function is given by an arithmetic averaging over local Green’s functions as

$$\hat{G}^{CPA}(\omega^+) = \int_{-\frac{x}{2}}^{\frac{x}{2}} d\epsilon_i \hat{G}^i(\omega^+) P_\epsilon(\epsilon_i). \quad (13)$$

Since the CPA maps the disordered problem onto a translationally invariant problem, a lattice Green's function may then be defined as

$$\hat{G}_{latt}(\vec{k}, \omega^+)^{-1} = \begin{pmatrix} \omega^+ + \mu - \epsilon(\vec{k}) - \Sigma_{11}^{CPA}(\omega^+) & -\Sigma_{12}^{CPA}(\omega^+) \\ -\Sigma_{21}^{CPA}(\omega^+) & \omega^+ - \mu + \epsilon(\vec{k}) - \Sigma_{22}^{CPA}(\omega^+) \end{pmatrix} \quad (14)$$

where the self-consistency condition is that the lattice self-energy is the same as the CPA self-energy, hence the CPA Green's function in term of average self-energy is given as

$$\hat{G}^{CPA}(\omega^+)^{-1} = \begin{pmatrix} \omega^+ + \mu - \Delta_{11}(\omega^+) - \Sigma_{11}^{CPA}(\omega^+) & -\Delta_{12}(\omega^+) - \Sigma_{12}^{CPA}(\omega^+) \\ -\Delta_{21}(\omega^+) - \Sigma_{21}^{CPA}(\omega^+) & \omega^+ - \mu - \Delta_{22}(\omega^+) - \Sigma_{22}^{CPA}(\omega^+) \end{pmatrix} \quad (15)$$

The equations are closed by observing that the \vec{k} summed lattice Green's function should be the CPA Green's function, i.e

$$\begin{aligned} \frac{1}{N_s} \sum_{\vec{k}} \hat{G}_{latt}(\vec{k}, \omega^+) &= \hat{G}^{CPA}(\omega^+) \\ \int_{-\infty}^{\infty} d\epsilon \rho_0(\epsilon) \hat{G}_{latt}(\epsilon, \omega^+) &= \hat{G}^{CPA}(\omega^+) \end{aligned} \quad (16)$$

where N_s and $\rho_0(\epsilon)$ are number of lattice sites and non-interacting density of state respectively. In practice, we follow the steps outlined below to obtain the converged order parameter and spectra.

1. Guess a hybridisation matrix $\hat{\Delta}(\omega^+)$ and n_i, Φ_i for each site. In practice, we choose either a previously converged solution or the non-interacting $\hat{\Delta}(\omega^+)$ with $n_i = 1$ and $\Phi_i = 1/2 \forall i$.
2. Given a hybridization, occupancy and order parameter, use equation (10) to calculate the host Green's function matrix, $\hat{\mathcal{G}}^i(\omega^+)$.
3. From equation (12), calculate pseudo-occupancy and pseudo-order parameter, n_{0i} and Φ_{0i} .
4. Now by using equations (4, 5, 8, 9, 11) calculate the regular and anomalous self-energies, $\Sigma_i(\omega^+)$ and $S_i(\omega^+)$.

5. Then by using equations (3, 6, 7), calculate impurity Green's function $\hat{G}^i(\omega^+)$, n_i, Φ_i for each site.
6. The disorder-averaged Green's function, $\hat{G}^{CPA}(\omega^+)$ is obtained using equation (13).
7. We consider the AHM on Bethe lattice of infinite connectivity at half filling, which is achieved by setting $\mu = -U/2$. For Bethe lattice the self-consistency condition is simply given by

$$\hat{\Delta}(\omega^+) = \frac{t^2 \sigma_z \hat{G}^{CPA}(\omega^+) \sigma_z}{4} \quad (17)$$

where σ_z is z component of Pauli's matrix. Using equation (17), a new hybridisation matrix $\hat{\Delta}$ is obtained.

8. If the hybridisation matrix $\hat{\Delta}(\omega^+)$ from step 7 and n_i, Φ_i from step 5 are equal (within a desired numerical tolerance) to the guess hybridisation matrix $\hat{\Delta}(\omega^+)$, n_i and Φ_i from step 1, then the iterations may be stopped, else the iterations continue until desired convergence is achieved.

The results obtained using the above-mentioned procedure will be denoted as IPTSC. We have also carried out mean-field calculations by 'turning off' the dynamical self-energies in equations 4 and 5. These results will be denoted as BdGMF. We present our results in the next section.

III. RESULTS AND DISCUSSION

A recent study of the clean AHM ($x = 0$) has shown that results obtained using NRG [7] compare well with those from the IPTSC method, thus indicating its reliability for the present problem. A total of 1600 lattice sites have been considered in our calculations. This implies that the impurity problem needs to be solved 1600 times for each DMFT iteration. A fully parallel implementation allows us to carry out efficient calculations in a wide-parameter range. This must be contrasted with previous state-of-the-art QMC calculations which have been carried out on a 8×8 square lattice, and results have been obtained at finite temperature on the imaginary frequency Matsubara axis. Thus not only are we able to consider much larger lattice sizes than previous works, but also obtain real frequency spectra directly at zero temperature.

We review the physics of the clean AHM within DMFT briefly. At half-filling ($n = 1$), it is well known that the AHM has two instabilities, namely superconductivity and charge-density wave (CDW). If the CDW instability is ignored, then the superconducting order parameter (Φ) becomes non-zero only for $U > U_{c1}$. The ground state is a normal metal for low interactions, while for $U > U_{c1}$, the single-particle spectrum develops a BCS superconducting gap. It is known from NRG calculations, that agree very well with IPTSC results, that with increasing U , the order parameter increases and saturates to a finite value as $U \rightarrow \infty$. However, this result does not agree with more recent CTQMC based calculations [8], which show that at large U , the order parameter decreases again, and vanishes beyond a certain $U = U_{c2}$. The contradicting results from NRG and CTQMC need further scrutiny. In this work, we will choose to take the NRG results as our benchmark.

A. Varying disorder; fixed interaction strength

In the clean case, the half-filling condition is maintained by choosing $\epsilon_i = 0$ and $\mu = -U/2$. For $x > 0$ the half-filling condition is again maintained through $\mu = -U/2$. The individual sites have site-energies that are distributed uniformly over $[-x/2, x/2]$, so there is very little probability that any single-site would have exactly $\epsilon_i = 0$. This implies that for a disordered AHM at a global half-filling condition, the individual sites are away from half-filling, hence the CDW instability need not be considered. In Fig. 1 we show the

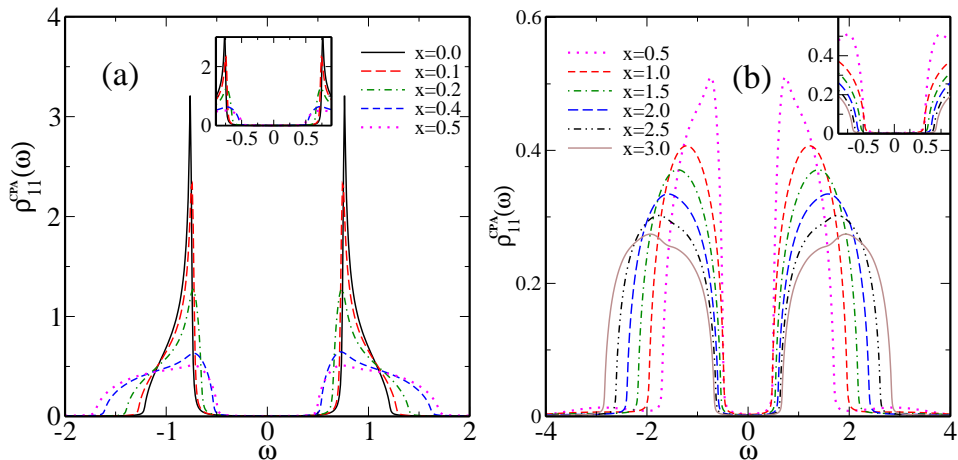


FIG. 1. (color online) Diagonal spectral function as function of frequency for different value of x at $U=2.0$: (a) low disorder results ($0 < x \leq 0.5$); (b) strong disorder results ($x \geq 0.5$). Insets show an expanded view of the low frequency gap region.

diagonal spectral function as a function of frequency for different values of disorder at a fixed interaction strength, namely $U = 2$. The panel (a) represents results for lower disorder ($x \leq 0.5$), while the panel (b) represents higher disorder ($x \geq 0.5$). The zero disorder case in the panel (a) represents the clean AHM result. The system has a superconducting gap E_g . Flanking the band edges are the sharp ‘coherence peaks’. With increasing disorder, the coherence peaks melt and change into broad features. The insets show an expanded view of the low frequency gap region.

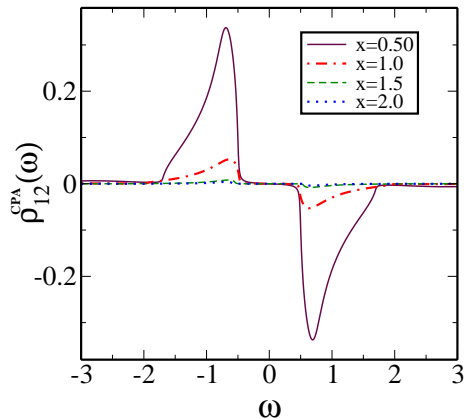


FIG. 2. Off diagonal spectral function for different values of x at a fixed $U = 2.0$.

To understand the nature of the gap, we need to analyse the off-diagonal spectral function. These are shown in Fig. 2, for disorder values varying from $x = 0.5$ to $x = 2$, and $U = 2$. It is seen clearly that the entire spectral weight decreases rapidly with increasing x , and finally goes to zero at $x \sim 1.5$. Comparing with Fig. 1, we see that the spectral gap does not close for any x . Thus, the system exhibits a superconductor-insulator transition (SIT) as a function of increasing disorder at a fixed U .

The effective averaged s-wave pairing amplitude, Φ^{CPA} is defined as

$$\Phi^{CPA} = \int_{-\infty}^{\infty} d\omega \frac{-\text{Im}(G_{12}^{CPA}(\omega^+))f(\omega)}{\pi}, \quad (18)$$

and computed using the mean field (dashed line) and IPTSC (solid line) methods for a fixed interaction strength. In Fig. 3, we show the spectral gap and the disorder-averaged superconducting order parameter as a function of disorder in the bottom and top panels respectively. It is observed that the gap decreases, reaches a minimum, and then increases with increasing disorder. This kind of behaviour of spectral gap with disorder is also re-

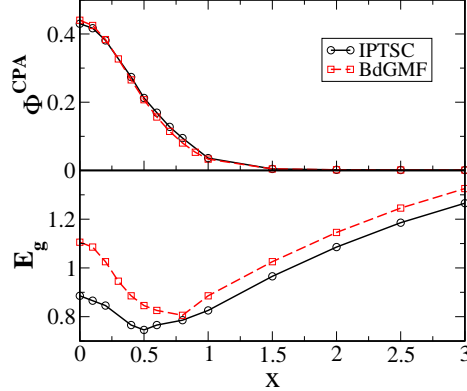


FIG. 3. Top panel: The disorder-averaged superconducting order parameter (solid line) as a function of x at $U = 2.0$. The dashed line is the BdGMF result for comparison. Bottom panel: The spectral gap as a function of disorder.

ported in [15, 16]. The order parameter, in contrast to the gap, decreases monotonically with increasing disorder and vanishes beyond $x \sim 1.5$. This result, which states that the superconducting state is destroyed beyond a critical disorder strength is consistent with previous QMC results, although the latter were obtained through extrapolation for finite size lattices. We show the BdGMF(CPA) result (dashed line) also in the same figure, and it is seen that the mean-field result and the full DMFT result hardly differ, indicating that local quantum fluctuations are not playing a significant role in the destruction of the superconducting state. Since the order parameter is finite for $x \lesssim 1.5$, the spectral gap is a superconducting gap, while for higher disorder ($x > 1.5$), since $\Phi = 0$, E_g represents an insulating gap. We also show the BdGMF(CPA) results for Φ and E_g in the same figure. It is seen that the spectral gap is overestimated by the static mean field approach for finite disorder, as was found at $x = 0$ [6].

The dependence of the gap on x is non-monotonic, and deserves some attention. For weak disorder, the gap decreases with increasing x , and this may be understood through the clean AHM. For $x = 0$, the spectral gap becomes smaller and asymmetric (about the chemical potential), with either increasing or decreasing the filling away from 1 [8]. Thus, we expect that with increasing disorder, since most sites would be off-half-filling, the spectral gap within CPA, arising as the arithmetic mean of the individual spectra, would decrease for weak disorder. The preceding argument assumes that the hybridization remains largely unaffected, which is true for weak disorder. However, for moderate and large disorder, the hybridization gets modified strongly, and the simple arithmetic averaging result cannot be

used to understand the increase in gap at larger disorder values ($x \gtrsim 1.5$). In order to understand the behaviour at large disorder, we will need to probe the distribution of the order parameter and gap over all the sites in the lattice. This is considered next.

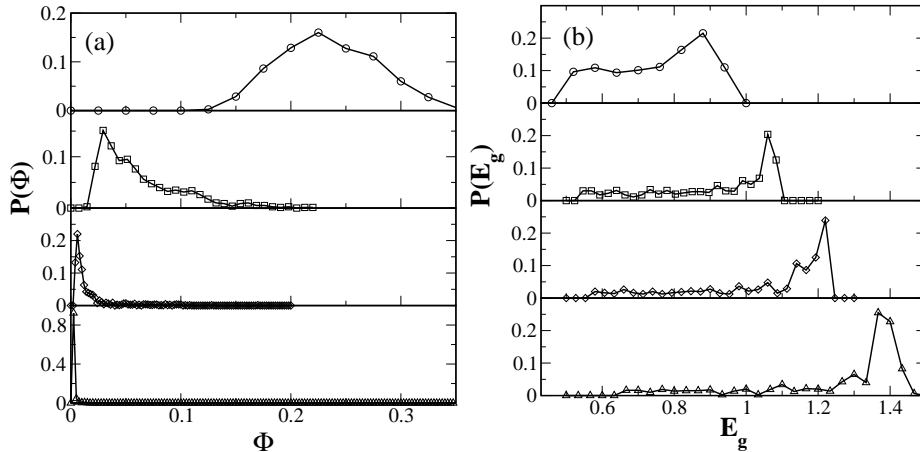


FIG. 4. Probability distribution of (a) local superconducting order parameter and (b) spectral gap for different values of $x = 0.5, 1.0, 1.5, 2.0$ (from top to bottom) at $U = 2.0$.

In Fig. 4(a), the probability distribution function of local superconducting order parameter (PDF-OP) for different values of x is shown. For small disorder, the PDF-OP is broad, and peaked moderately at a certain typical value of Φ . With increasing x the typical Φ decreases sharply and the PDF-OP narrows down considerably. This indicates that, while in the weak disorder limit, arithmetic averaging may be used, in the strong disorder limit the typical value will manifest macroscopically. This is also reflected in the probability distribution function for spectral gap (PDF-SG). As expected, the PDF-SG is also broad at weak disorder and narrows considerably at large disorder. In fact, since the weight contained in the peak is almost more than 50%, most of the sites will have a gap in the neighbourhood of the gap value corresponding to the peak. Since the peak occurs at higher values of the gap with increasing x , the gap in the CPA spectral function, shown in the bottom panel of Fig. 3, increases with increasing x . In previous literature based on BdGMF or QMC of finite lattices incorporating inhomogeneous order parameters, this increase in gap as a function of x has been attributed to decrease in localization length. Our results are based on the CPA, which is known to ignore localization effects. Thus we suggest that the arguments based on PDF are sufficient, and localization physics need not be invoked to explain the increase of the insulating gap. A more sophisticated treatment of this problem could be through typical medium theory, and subsequently statistical DMFT. Although the latter has been carried

out [12], this specific issue has not been addressed.

B. Fixed disorder; varying interaction strength

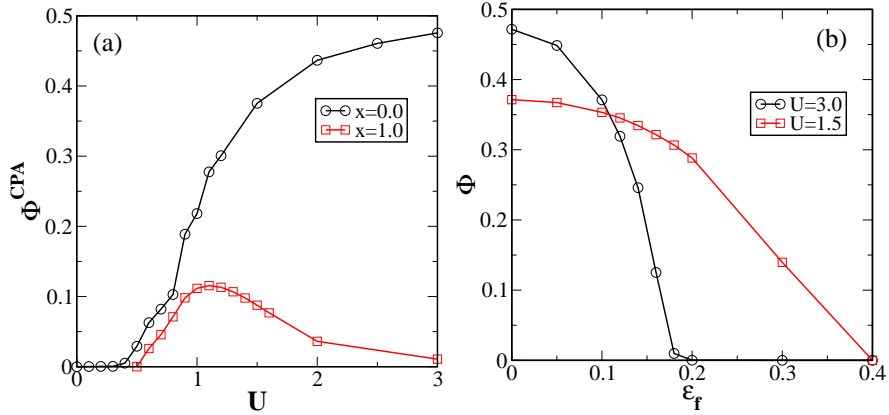


FIG. 5. (a) Superconducting order parameter of the disordered AHM as a function of U at $x = 0, 1.0$; (b) The Φ of the clean AHM as a function of site-energy ϵ_f for fixed $U = 1.5$ and 3.0 .

We have considered the behaviour of physical quantities as a function of disorder at a fixed interaction strength. Now, we show the order parameter as a function of U at a fixed disorder. In the Fig. 5(a), the superconducting order parameter computed at $x = 0$ and $x = 1.0$ is shown as a function of U . For the clean case ($x = 0$), as mentioned before, Φ increases and eventually saturates with increasing U . However, at finite disorder, Φ^{CPA} increases, reaches a maximum and subsequently decreases. Thus when we turn on disorder, the order parameter dependence on U changes qualitatively. This can again be understood very simply from the clean AHM result, that at a fixed U , Φ decreases with increasing particle-hole asymmetry defined by $\eta = 1 - 2|(\epsilon_i - \mu)/U|$, as shown in Fig. 5(b). For a larger U , the decrease of Φ with increasing η is much more rapid. Increasing site-disorder implies creating a greater number of sites with large η , which would have a smaller Φ as compared to the sites with $\eta \sim 0$. Thus, with increasing interaction strength, and a fixed disorder concentration, the superconducting order parameter should decrease, and is indeed obtained.

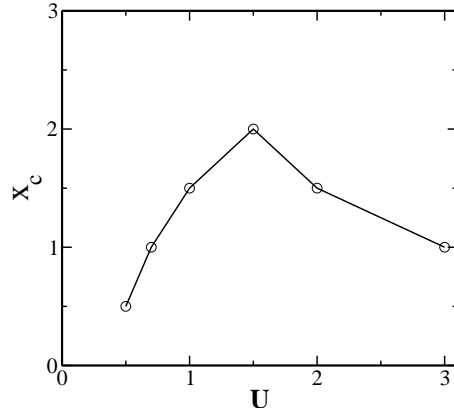


FIG. 6. The critical disorder $x_c(U)$ beyond which the superconducting state is completely destroyed is shown as a function of U .

C. ‘Phase diagram’

The variation of the spectral gap and the superconducting order parameter, shown in Fig. 3, was for a specific interaction strength, namely $U = 2.0$. We have repeated our calculations for various other U values, and could thus find the critical disorder strength $x_c(U)$, beyond which the superconducting state is completely destroyed. As shown in Fig. 6, we find that for large U , the $x_c(U)$ decreases with increasing the interaction strength. This kind of behaviour is also seen in QMC calculations of finite lattices through extrapolation [17]. The superconducting state persists to higher disorder values with increasing U in the weak to moderate coupling regime, in contrast to the strong coupling regime.

IV. CONCLUSIONS

In this paper, we have studied the effects of site-disorder on a s-wave superconducting state as represented by an inhomogeneous attractive Hubbard model. Our theoretical approach combines DMFT with IPTSC as an impurity solver and the CPA. Detailed studies of (a) the clean system away from half-filling and (b) probability distributions of the spectral gap and order parameter have been carried out. We have computed single-particle quantities such as the diagonal and off-diagonal spectral functions in the disorder- U plane. Using these, we obtained the spectral gap, superconducting order parameter and their probability distributions for different values of disorder and interaction strength. Some of our results agree qualitatively with those of previous studies [15–17]. These include the non-monotonic

dependence of the spectral gap on the interaction strength, the destruction of the superconducting state with disorder and a concomitant superconductor-insulator transition. These studies [15–17] were carried out on two-dimensional lattices, while our work is within DMFT. Thus, we conclude that dimensionality has little role to play in these results. We further argue that our results may be explained by utilizing particle-hole asymmetry and disorder induced probability distributions, with no necessity to invoke localization physics.

In order to probe localization physics within local approaches, one must ideally incorporate short-range correlations using techniques such as typical medium-dynamical cluster approximation [21]. The extension of our results to finite temperature and general fillings would pave the way to comparison with experiments.

V. ACKNOWLEDGMENTS

The authors thank CSIR, India and JNCASR, India for funding this research.

-
- [1] P. A. Lee and T. V. Ramakrishnan, *Rev. Mod. Phys.* **57**, 287 (1985).
 - [2] D. Belitz and T. R. Kirkpatrick, *Rev. Mod. Phys.* **66**, 261 (1994).
 - [3] Mintu Mondal *et al*, *Phys. Rev. Lett.* **106**, 047001 (2011).
 - [4] Madhavi Chand *et al*, *Phys. Rev. B* **85**, 014508 (2012).
 - [5] R. Crane, N. P. Armitage, A. Johansson, G. Sambandamurthy, D. Shahar, G. Gruner, *Phys. Rev. B* **75**, 184530 (2007).
 - [6] A. Garg, H. R. Krishnamurthy, and M. Randeria, *Phys. Rev. B* **72**, 024517 (2005).
 - [7] J. Bauer, A. C. Hewson, and N. Dupuis, *Phys. Rev. B* **79**, 214518 (2009).
 - [8] Akihisa Koga, Philipp Werner, *Phys. Rev. A* **84**, 023638 (2011).
 - [9] A. Georges, G. Kotliar, W. Krauth, and M. J. Rozenberg, *Rev. Mod. Phys.* **68**, 13 (1996).
 - [10] G. Kotliar, D. Vollhardt, *Physics Today*, (2004).
 - [11] D. Vollhardt, *AIP Conference Proceedings* **1297**, 339 (2010) .
 - [12] Masaru Sakaida, Kazuto Noda, and Norio Kawakami, *J. Phys. Soc. Japan* **82** 074715 (2013).
 - [13] P. W. Anderson, *J. Phys. Chem. Solids* **11**, 26 (1959).
 - [14] A. A. Abrikosov and L. P. Gorkov, *Sov. Phys. JETP* **9**, 220 (1959).

- [15] A. Ghosal, M. Randeria and N. Trivedi, Phys. Rev. B **65**, 014501 (2001).
- [16] Sanjeev Kumar and Prabuddha B. Chakraborty, arXiv:1302.1967.
- [17] R. T. Scalettar, N. Trivedi, C. Huscroft, Phys. Rev. B **59**, 4364 (1999).
- [18] R. J. Elliott, J. A. Krumhansl, and P. L. Leath, Rev. Mod. Phys. **46**, 465 (1974).
- [19] V. Janis and D. Vollhardt, Phys. Rev. B **46**, 15712 (1992).
- [20] M. Potthoff and M. Balzer, Phys. Rev. B **75**, 125112 (2007).
- [21] Chinedu E. Ekuma *et al*, arXiv:1306.5712.